University of Groningen

Search for the semileptonic decays Ds+ →k1 (1270)0e+ve and Ds+ →b1 (1235)0e+ve

BESIII Collaboration; Kalantar-Nayestanaki, N.; Kappert, Rosa; Kavatsyuk, M.; Messchendorp, J.; Rodin, Viktor

Published in:
Physical Review D

DOI:
10.1103/PhysRevD.108.112002

IMPORTANT NOTE: You are advised to consult the publisher's version (publisher's PDF) if you wish to cite from it. Please check the document version below.

Document Version
Publisher's PDF, also known as Version of record

Publication date:
2023

Link to publication in University of Groningen/UMCG research database

Citation for published version (APA):
BESIII Collaboration, Kalantar-Nayestanaki, N., Kappert, R., Kavatsyuk, M., Messchendorp, J., & Rodin, V. (2023). Search for the semileptonic decays Ds+ →k1 (1270)0e+ve and Ds+ →b1 (1235)0e+ve. *Physical Review D*, *108*(11), Article 112002. https://doi.org/10.1103/PhysRevD.108.112002

Copyright
Other than for strictly personal use, it is not permitted to download or to forward/distribute the text or part of it without the consent of the author(s) and/or copyright holder(s), unless the work is under an open content license (like Creative Commons).

The publication may also be distributed here under the terms of Article 25fa of the Dutch Copyright Act, indicated by the “Taverne” license. More information can be found on the University of Groningen website: https://www.rug.nl/library/open-access/self-archiving-pure/taverne-amendment.

Take-down policy
If you believe that this document breaches copyright please contact us providing details, and we will remove access to the work immediately and investigate your claim.

Downloaded from the University of Groningen/UMCG research database (Pure): http://www.rug.nl/research/portal. For technical reasons the number of authors shown on this cover page is limited to 10 maximum.

Download date: 01-02-2024

Search for the semileptonic decays $D_s^+ \to K_1(1270)^0 e^+ \nu_e$ and $D_s^+ \to b_1(1235)^0 e^+ \nu_e$

M. Ablikim,[1] M. N. Achasov,[5,b] P. Adlarson,[75] X. C. Ai,[81] R. Aliberti,[36] A. Amoroso,[74a,74c] M. R. An,[40] Q. An,[71,58] Y. Bai,[57]
O. Bakina,[37] I. Balossino,[30a] Y. Ban,[47,g] V. Batozskaya,[1,45] K. Begzsuren,[33] N. Berger,[36] M. Berlowski,[45] M. Bertani,[29a]
D. Bettoni,[30a] F. Bianchi,[74a,74c] E. Bianco,[74a,74c] A. Bortone,[74a,74c] I. Boyko,[37] R. A. Briere,[6] A. Brueggemann,[68] H. Cai,[76]
X. Cai,[1,58] A. Calcaterra,[29a] G. F. Cao,[1,63] N. Cao,[1,63] S. A. Cetin,[62a] J. F. Chang,[1,58] T. T. Chang,[77] W. L. Chang,[1,63]
G. R. Che,[44] G. Chelkov,[37,a] C. Chen,[44] Chao Chen,[55] G. Chen,[1] H. S. Chen,[1,63] M. L. Chen,[1,58,63] S. J. Chen,[43]
S. M. Chen,[61] T. Chen,[1,63] X. R. Chen,[32,63] X. T. Chen,[1,63] Y. B. Chen,[1,58] Y. Q. Chen,[35] Z. J. Chen,[26,h] W. S. Cheng,[74c]
S. K. Choi,[11] X. Chu,[44] G. Cibinetto,[30a] S. C. Coen,[4] F. Cossio,[74c] J. J. Cui,[50] H. L. Dai,[1,58] J. P. Dai,[79] A. Dbeyssi,[19]
R. E. de Boer,[4] D. Dedovich,[37] Z. Y. Deng,[1] A. Denig,[36] I. Denysenko,[37] M. Destefanis,[74a,74c] F. De Mori,[74a,74c] B. Ding,[66,1]
X. X. Ding,[47,g] Y. Ding,[41] Y. Ding,[35] J. Dong,[1,58] L. Y. Dong,[1,63] M. Y. Dong,[1,58,63] X. Dong,[76] M. C. Du,[1] S. X. Du,[81]
Z. H. Duan,[43] P. Egorov,[37,a] Y. L. Fan,[76] J. Fang,[1,58] S. S. Fang,[1,63] W. X. Fang,[1] Y. Fang,[1] R. Farinelli,[30a] L. Fava,[74b,74c]
F. Feldbauer,[4] G. Felici,[29a] C. Q. Feng,[71,58] J. H. Feng,[59] K. Fischer,[69] M. Fritsch,[4] C. Fritzsch,[68] C. D. Fu,[1] J. L. Fu,[63]
Y. W. Fu,[1] H. Gao,[63] Y. N. Gao,[47,g] Yang Gao,[71,58] S. Garbolino,[74c] I. Garzia,[30a,30b] P. T. Ge,[76] Z. W. Ge,[43] C. Geng,[59]
E. M. Gersabeck,[67] A. Gilman,[69] K. Goetzen,[14] L. Gong,[41] W. X. Gong,[1,58] W. Gradl,[36] S. Gramigna,[30a,30b] M. Greco,[74a,74c]
M. H. Gu,[1,58] Y. T. Gu,[16] C. Y. Guan,[1,63] Z. L. Guan,[23] A. Q. Guo,[32,63] L. B. Guo,[42] M. J. Guo,[50] R. P. Guo,[49] Y. P. Guo,[13,f]
A. Guskov,[37,a] T. T. Han,[50] W. Y. Han,[40] X. Q. Hao,[20] F. A. Harris,[65] K. K. He,[55] K. L. He,[1,63] F. H. H. Heinsius,[4]
C. H. Heinz,[36] Y. K. Heng,[1,58,63] C. Herold,[60] T. Holtmann,[4] P. C. Hong,[13,f] G. Y. Hou,[1,63] X. T. Hou,[1,63] Y. R. Hou,[63]
Z. L. Hou,[1] H. M. Hu,[1,63] J. F. Hu,[56,i] T. Hu,[1,58,63] Y. Hu,[1] G. S. Huang,[71,58] K. X. Huang,[59] L. Q. Huang,[32,63] X. T. Huang,[50]
Y. P. Huang,[1] T. Hussain,[73] N. Hüsken,[28,36] W. Imoehl,[28] M. Irshad,[71,58] J. Jackson,[28] S. Jaeger,[4] S. Janchiv,[33] J. H. Jeong,[11]
Q. Ji,[1] Q. P. Ji,[20] X. B. Ji,[1,63] X. L. Ji,[1,58] Y. Y. Ji,[50] X. Q. Jia,[50] Z. K. Jia,[71,58] H. J. Jiang,[76] P. C. Jiang,[47,g] S. S. Jiang,[40]
T. J. Jiang,[17] X. S. Jiang,[1,58,63] Y. Jiang,[63] J. B. Jiao,[50] Z. Jiao,[24] S. Jin,[43] Y. Jin,[66] M. Q. Jing,[1,63] T. Johansson,[75] X. K.,[1]
S. Kabana,[34] N. Kalantar-Nayestanaki,[64] X. L. Kang,[10] X. S. Kang,[41] R. Kappert,[64] M. Kavatsyuk,[64] B. C. Ke,[81]
A. Khoukaz,[68] R. Kiuchi,[1] R. Kliemt,[14] O. B. Kolcu,[62a] B. Kopf,[4] M. K. Kuessner,[4] A. Kupsc,[45,75] W. Kühn,[38] J. J. Lane,[67]
P. Larin,[19] A. Lavania,[27] L. Lavezzi,[74a,74c] T. T. Lei,[71,k] Z. H. Lei,[71,58] H. Leithoff,[36] M. Lellmann,[36] T. Lenz,[36] C. Li,[44]
C. Li,[48] C. H. Li,[40] Cheng Li,[71,58] D. M. Li,[81] F. Li,[1,58] G. Li,[1] H. Li,[71,58] H. B. Li,[1,63] H. J. Li,[20] H. N. Li,[56,i] Hui Li,[44]
J. R. Li,[61] J. S. Li,[59] J. W. Li,[50] K. L. Li,[20] Ke Li,[1] L. J. Li,[1,63] L. K. Li,[1] Lei Li,[3] M. H. Li,[44] P. R. Li,[39,j,k] Q. X. Li,[50]
S. X. Li,[13] T. Li,[50] W. D. Li,[1,63] W. G. Li,[1] X. H. Li,[71,58] X. L. Li,[50] Xiaoyu Li,[1,63] Y. G. Li,[47,g] Z. J. Li,[59] Z. X. Li,[16]
C. Liang,[43] H. Liang,[35] H. Liang,[1,63] H. Liang,[71,58] Y. F. Liang,[54] Y. T. Liang,[32,63] G. R. Liao,[15] L. Z. Liao,[50] Y. P. Liao,[1,63]
J. Libby,[27] A. Limphirat,[60] D. X. Lin,[32,63] T. Lin,[1] B. J. Liu,[1] B. X. Liu,[76] C. Liu,[35] C. X. Liu,[1] F. H. Liu,[53] Fang Liu,[1]
Feng Liu,[7] G. M. Liu,[56,i] H. Liu,[39,j,k] H. B. Liu,[16] H. M. Liu,[1,63] Huanhuan Liu,[1] Huihui Liu,[22] J. B. Liu,[71,58] J. L. Liu,[72]
J. Y. Liu,[1,63] K. Liu,[1] K. Y. Liu,[41] Ke Liu,[23] L. Liu,[71,58] L. C. Liu,[44] Lu Liu,[44] M. H. Liu,[13,f] P. L. Liu,[1] Q. Liu,[63] S. B. Liu,[71,58]
T. Liu,[13,f] W. K. Liu,[44] W. M. Liu,[71,58] X. Liu,[39,j,k] Y. Liu,[39,j,k] Y. Liu,[81] Y. B. Liu,[44] Z. A. Liu,[1,58,63] Z. Q. Liu,[50]
X. C. Lou,[1,58,63] F. X. Lu,[59] H. J. Lu,[24] J. G. Lu,[1,58] X. L. Lu,[1] Y. Lu,[8] Y. P. Lu,[1,58] Z. H. Lu,[1,63] C. L. Luo,[42] M. X. Luo,[80]
T. Luo,[13,f] X. L. Luo,[1,58] X. R. Lyu,[63] Y. F. Lyu,[44] F. C. Ma,[41] H. L. Ma,[1] J. L. Ma,[1,63] L. L. Ma,[50] M. M. Ma,[1,63] Q. M. Ma,[1]
R. Q. Ma,[1,63] R. T. Ma,[63] X. Y. Ma,[1,58] Y. Ma,[47,g] Y. M. Ma,[32] F. E. Maas,[19] M. Maggiora,[74a,74c] S. Malde,[69] Q. A. Malik,[73]
A. Mangoni,[29b] Y. J. Mao,[47,g] Z. P. Mao,[1] S. Marcello,[74a,74c] Z. X. Meng,[66] J. G. Messchendorp,[14,64] G. Mezzadri,[30a]
H. Miao,[1,63] T. J. Min,[43] R. E. Mitchell,[28] X. H. Mo,[1,58,63] N. Yu. Muchnoi,[5,b] Y. Nefedov,[37] F. Nerling,[19,d] I. B. Nikolaev,[5,b]
Z. Ning,[1,58] S. Nisar,[12,l] Y. Niu,[50] S. L. Olsen,[63] Q. Ouyang,[1,58,63] S. Pacetti,[29b,29c] X. Pan,[55] Y. Pan,[57] A. Pathak,[35]
P. Patteri,[29a] Y. P. Pei,[71,58] M. Pelizaeus,[4] H. P. Peng,[71,58] K. Peters,[14,d] J. L. Ping,[42] R. G. Ping,[1,63] S. Plura,[36] S. Pogodin,[37]
V. Prasad,[34] F. Z. Qi,[1] H. Qi,[71,58] H. R. Qi,[61] M. Qi,[43] T. Y. Qi,[13,f] S. Qian,[1,58] W. B. Qian,[63] C. F. Qiao,[63] J. J. Qin,[72]
L. Q. Qin,[15] X. P. Qin,[13,f] X. S. Qin,[50] Z. H. Qin,[1,58] J. F. Qiu,[1] S. Q. Qu,[61] C. F. Redmer,[36] K. J. Ren,[40] A. Rivetti,[74c]
V. Rodin,[64] M. Rolo,[74c] G. Rong,[1,63] Ch. Rosner,[19] S. N. Ruan,[44] N. Salone,[45] A. Sarantsev,[37,c] Y. Schelhaas,[36]
K. Schoenning,[75] M. Scodeggio,[30a,30b] K. Y. Shan,[13,f] W. Shan,[25] X. Y. Shan,[71,58] J. F. Shangguan,[55] L. G. Shao,[1,63]
M. Shao,[71,58] C. P. Shen,[13,f] H. F. Shen,[1,63] W. H. Shen,[63] X. Y. Shen,[1,63] B. A. Shi,[63] H. C. Shi,[71,58] J. L. Shi,[13] J. Y. Shi,[1]
Q. Q. Shi,[55] R. S. Shi,[1,63] X. Shi,[1,58] J. J. Song,[20] T. Z. Song,[59] W. M. Song,[35,1] Y. J. Song,[13] Y. X. Song,[47,g] S. Sosio,[74a,74c]
S. Spataro,[74a,74c] F. Stieler,[36] Y. J. Su,[63] G. B. Sun,[76] G. X. Sun,[1] H. Sun,[63] H. K. Sun,[1] J. F. Sun,[20] K. Sun,[61] L. Sun,[76]
S. S. Sun,[1,63] T. Sun,[1,63] W. Y. Sun,[35] Y. Sun,[10] Y. J. Sun,[71,58] Y. Z. Sun,[1] Z. T. Sun,[50] Y. X. Tan,[71,58] C. J. Tang,[54] G. Y. Tang,[1]
J. Tang,[59] Y. A. Tang,[76] L. Y. Tao,[72] Q. T. Tao,[26,h] M. Tat,[69] J. X. Teng,[71,58] V. Thoren,[75] W. H. Tian,[59] W. H. Tian,[52]
Y. Tian,[32,63] Z. F. Tian,[76] I. Uman,[62b] S. J. Wang,[50] B. Wang,[1] B. L. Wang,[63] Bo Wang,[71,58] C. W. Wang,[43] D. Y. Wang,[47,g]
F. Wang,[72] H. J. Wang,[39,j,k] H. P. Wang,[1,63] J. P. Wang,[50] K. Wang,[1,58] L. L. Wang,[1] M. Wang,[50] Meng Wang,[1,63]
S. Wang,[39,j,k] S. Wang,[13,f] T. Wang,[13,f] T. J. Wang,[44] W. Wang,[72] W. Wang,[59] W. P. Wang,[71,58] X. Wang,[47,g] X. F. Wang,[39,j,k]

2470-0010/2023/108(11)/112002(11)

Published by the American Physical Society

X. J. Wang,[40] X. L. Wang,[13,f] Y. Wang,[61] Y. D. Wang,[46] Y. F. Wang,[1,58,63] Y. H. Wang,[48] Y. N. Wang,[46] Y. Q. Wang,[1]
Yaqian Wang,[18,1] Yi Wang,[61] Z. Wang,[1,58] Z. L. Wang,[72] Z. Y. Wang,[1,63] Ziyi Wang,[63] D. Wei,[70] D. H. Wei,[15] F. Weidner,[68]
S. P. Wen,[1] C. W. Wenzel,[4] U. W. Wiedner,[4] G. Wilkinson,[69] M. Wolke,[75] L. Wollenberg,[4] C. Wu,[40] J. F. Wu,[1,63] L. H. Wu,[1]
L. J. Wu,[1,63] X. Wu,[13,f] X. H. Wu,[35] Y. Wu,[71] Y. J. Wu,[32] Z. Wu,[1,58] L. Xia,[71,58] X. M. Xian,[40] T. Xiang,[47,g] D. Xiao,[39,j,k]
G. Y. Xiao,[43] H. Xiao,[13,f] S. Y. Xiao,[1] Y. L. Xiao,[13,f] Z. J. Xiao,[42] C. Xie,[43] X. H. Xie,[47,g] Y. Xie,[50] Y. G. Xie,[1,58] Y. H. Xie,[7]
Z. P. Xie,[71,58] T. Y. Xing,[1,63] C. F. Xu,[1,63] C. J. Xu,[59] G. F. Xu,[1] H. Y. Xu,[66] Q. J. Xu,[17] Q. N. Xu,[31] W. Xu,[1,63] W. L. Xu,[66]
X. P. Xu,[55] Y. C. Xu,[78] Z. P. Xu,[43] Z. S. Xu,[63] F. Yan,[13,f] L. Yan,[13,f] W. B. Yan,[71,58] W. C. Yan,[81] X. Q. Yan,[1] H. J. Yang,[51,e]
H. L. Yang,[35] H. X. Yang,[1] Tao Yang,[1] Y. Yang,[13,f] Y. F. Yang,[44] Y. X. Yang,[1,63] Yifan Yang,[1,63] Z. W. Yang,[39,j,k] Z. P. Yao,[50]
M. Ye,[1,58] M. H. Ye,[9] J. H. Yin,[1] Z. Y. You,[59] B. X. Yu,[1,58,63] C. X. Yu,[44] G. Yu,[1,63] J. S. Yu,[26,h] T. Yu,[72] X. D. Yu,[47,g]
C. Z. Yuan,[1,63] L. Yuan,[2] S. C. Yuan,[1] X. Q. Yuan,[1] Y. Yuan,[1,63] Z. Y. Yuan,[59] C. X. Yue,[40] A. A. Zafar,[73] F. R. Zeng,[50]
X. Zeng,[13,f] Y. Zeng,[26,h] Y. J. Zeng,[1,63] X. Y. Zhai,[35] Y. C. Zhai,[50] Y. H. Zhan,[59] A. Q. Zhang,[1,63] B. L. Zhang,[1,63]
B. X. Zhang,[1] D. H. Zhang,[44] G. Y. Zhang,[20] H. Zhang,[71] H. H. Zhang,[59] H. H. Zhang,[35] H. Q. Zhang,[1,58,63] H. Y. Zhang,[1,58]
J. J. Zhang,[52] J. L. Zhang,[21] J. Q. Zhang,[42] J. W. Zhang,[1,58,63] J. X. Zhang,[39,j,k] J. Y. Zhang,[1] J. Z. Zhang,[1,63] Jianyu Zhang,[63]
Jiawei Zhang,[1,63] L. M. Zhang,[61] L. Q. Zhang,[59] Lei Zhang,[43] P. Zhang,[1] Q. Y. Zhang,[40,81] Shuihan Zhang,[1,63]
Shulei Zhang,[26,h] X. D. Zhang,[46] X. M. Zhang,[1] X. Y. Zhang,[55] X. Y. Zhang,[50] Y. Zhang,[72] Y. Zhang,[69] Y. T. Zhang,[81]
Y. H. Zhang,[1,58] Yan Zhang,[71,58] Yao Zhang,[1] Z. H. Zhang,[1] Z. L. Zhang,[35] Z. Y. Zhang,[44] Z. Y. Zhang,[76] G. Zhao,[1]
J. Zhao,[40] J. Y. Zhao,[1,63] J. Z. Zhao,[1,58] Lei Zhao,[71,58] Ling Zhao,[1] M. G. Zhao,[44] S. J. Zhao,[81] Y. B. Zhao,[1,58] Y. X. Zhao,[32,63]
Z. G. Zhao,[71,58] A. Zhemchugov,[37,a] B. Zheng,[72] J. P. Zheng,[1,58] W. J. Zheng,[1,63] Y. H. Zheng,[63] B. Zhong,[42] X. Zhong,[59]
H. Zhou,[50] L. P. Zhou,[1,63] X. Zhou,[76] X. K. Zhou,[7] X. R. Zhou,[71,58] X. Y. Zhou,[40] Y. Z. Zhou,[13,f] J. Zhu,[44] K. Zhu,[1]
K. J. Zhu,[1,58,63] L. Zhu,[35] L. X. Zhu,[63] S. H. Zhu,[70] S. Q. Zhu,[43] T. J. Zhu,[13,f] W. J. Zhu,[13,f] Y. C. Zhu,[71,58] Z. A. Zhu,[1,63]
J. H. Zou,[1] and J. Zu[71,58]

(BESIII Collaboration)

[1]*Institute of High Energy Physics, Beijing 100049, People's Republic of China*
[2]*Beihang University, Beijing 100191, People's Republic of China*
[3]*Beijing Institute of Petrochemical Technology, Beijing 102617, People's Republic of China*
[4]*Bochum Ruhr-University, D-44780 Bochum, Germany*
[5]*Budker Institute of Nuclear Physics SB RAS (BINP), Novosibirsk 630090, Russia*
[6]*Carnegie Mellon University, Pittsburgh, Pennsylvania 15213, USA*
[7]*Central China Normal University, Wuhan 430079, People's Republic of China*
[8]*Central South University, Changsha 410083, People's Republic of China*
[9]*China Center of Advanced Science and Technology, Beijing 100190, People's Republic of China*
[10]*China University of Geosciences, Wuhan 430074, People's Republic of China*
[11]*Chung-Ang University, Seoul, 06974, Republic of Korea*
[12]*COMSATS University Islamabad, Lahore Campus, Defence Road,*
Off Raiwind Road, 54000 Lahore, Pakistan
[13]*Fudan University, Shanghai 200433, People's Republic of China*
[14]*GSI Helmholtzcentre for Heavy Ion Research GmbH, D-64291 Darmstadt, Germany*
[15]*Guangxi Normal University, Guilin 541004, People's Republic of China*
[16]*Guangxi University, Nanning 530004, People's Republic of China*
[17]*Hangzhou Normal University, Hangzhou 310036, People's Republic of China*
[18]*Hebei University, Baoding 071002, People's Republic of China*
[19]*Helmholtz Institute Mainz, Staudinger Weg 18, D-55099 Mainz, Germany*
[20]*Henan Normal University, Xinxiang 453007, People's Republic of China*
[21]*Henan University, Kaifeng 475004, People's Republic of China*
[22]*Henan University of Science and Technology, Luoyang 471003, People's Republic of China*
[23]*Henan University of Technology, Zhengzhou 450001, People's Republic of China*
[24]*Huangshan College, Huangshan 245000, People's Republic of China*
[25]*Hunan Normal University, Changsha 410081, People's Republic of China*
[26]*Hunan University, Changsha 410082, People's Republic of China*
[27]*Indian Institute of Technology Madras, Chennai 600036, India*
[28]*Indiana University, Bloomington, Indiana 47405, USA*
[29a]*INFN Laboratori Nazionali di Frascati, I-00044, Frascati, Italy*
[29b]*INFN Sezione di Perugia, I-06100, Perugia, Italy*

[29c]*University of Perugia, I-06100, Perugia, Italy*
[30a]*INFN Sezione di Ferrara, I-44122, Ferrara, Italy*
[30b]*University of Ferrara, I-44122, Ferrara, Italy*
[31]*Inner Mongolia University, Hohhot 010021, People's Republic of China*
[32]*Institute of Modern Physics, Lanzhou 730000, People's Republic of China*
[33]*Institute of Physics and Technology, Peace Avenue 54B, Ulaanbaatar 13330, Mongolia*
[34]*Instituto de Alta Investigación, Universidad de Tarapacá, Casilla 7D, Arica 1000000, Chile*
[35]*Jilin University, Changchun 130012, People's Republic of China*
[36]*Johannes Gutenberg University of Mainz, Johann-Joachim-Becher-Weg 45, D-55099 Mainz, Germany*
[37]*Joint Institute for Nuclear Research, 141980 Dubna, Moscow region, Russia*
[38]*Justus-Liebig-Universitaet Giessen, II. Physikalisches Institut, Heinrich-Buff-Ring 16, D-35392 Giessen, Germany*
[39]*Lanzhou University, Lanzhou 730000, People's Republic of China*
[40]*Liaoning Normal University, Dalian 116029, People's Republic of China*
[41]*Liaoning University, Shenyang 110036, People's Republic of China*
[42]*Nanjing Normal University, Nanjing 210023, People's Republic of China*
[43]*Nanjing University, Nanjing 210093, People's Republic of China*
[44]*Nankai University, Tianjin 300071, People's Republic of China*
[45]*National Centre for Nuclear Research, Warsaw 02-093, Poland*
[46]*North China Electric Power University, Beijing 102206, People's Republic of China*
[47]*Peking University, Beijing 100871, People's Republic of China*
[48]*Qufu Normal University, Qufu 273165, People's Republic of China*
[49]*Shandong Normal University, Jinan 250014, People's Republic of China*
[50]*Shandong University, Jinan 250100, People's Republic of China*
[51]*Shanghai Jiao Tong University, Shanghai 200240, People's Republic of China*
[52]*Shanxi Normal University, Linfen 041004, People's Republic of China*
[53]*Shanxi University, Taiyuan 030006, People's Republic of China*
[54]*Sichuan University, Chengdu 610064, People's Republic of China*
[55]*Soochow University, Suzhou 215006, People's Republic of China*
[56]*South China Normal University, Guangzhou 510006, People's Republic of China*
[57]*Southeast University, Nanjing 211100, People's Republic of China*
[58]*State Key Laboratory of Particle Detection and Electronics, Beijing 100049, Hefei 230026, People's Republic of China*
[59]*Sun Yat-Sen University, Guangzhou 510275, People's Republic of China*
[60]*Suranaree University of Technology, University Avenue 111, Nakhon Ratchasima 30000, Thailand*
[61]*Tsinghua University, Beijing 100084, People's Republic of China*
[62a]*Turkish Accelerator Center Particle Factory Group, Istinye University, 34010, Istanbul, Turkey*
[62b]*Near East University, Nicosia, North Cyprus, 99138, Mersin 10, Turkey*
[63]*University of Chinese Academy of Sciences, Beijing 100049, People's Republic of China*
[64]*University of Groningen, NL-9747 AA Groningen, The Netherlands*
[65]*University of Hawaii, Honolulu, Hawaii 96822, USA*
[66]*University of Jinan, Jinan 250022, People's Republic of China*
[67]*University of Manchester, Oxford Road, Manchester, M13 9PL, United Kingdom*
[68]*University of Muenster, Wilhelm-Klemm-Strasse 9, 48149 Muenster, Germany*
[69]*University of Oxford, Keble Road, Oxford OX13RH, United Kingdom*
[70]*University of Science and Technology Liaoning, Anshan 114051, People's Republic of China*
[71]*University of Science and Technology of China, Hefei 230026, People's Republic of China*
[72]*University of South China, Hengyang 421001, People's Republic of China*
[73]*University of the Punjab, Lahore-54590, Pakistan*
[74a]*University of Turin and INFN, University of Turin, I-10125, Turin, Italy*
[74b]*University of Eastern Piedmont, I-15121, Alessandria, Italy*
[74c]*INFN, I-10125, Turin, Italy*
[75]*Uppsala University, Box 516, SE-75120 Uppsala, Sweden*
[76]*Wuhan University, Wuhan 430072, People's Republic of China*
[77]*Xinyang Normal University, Xinyang 464000, People's Republic of China*
[78]*Yantai University, Yantai 264005, People's Republic of China*
[79]*Yunnan University, Kunming 650500, People's Republic of China*

[80]*Zhejiang University, Hangzhou 310027, People's Republic of China*
[81]*Zhengzhou University, Zhengzhou 450001, People's Republic of China*

(Received 8 September 2023; accepted 1 November 2023; published 4 December 2023)

By analyzing 7.33 fb^{-1} of e^+e^- collision data collected at center-of-mass energies between 4.128 and 4.226 GeV with the BESIII detector, we search for the semileptonic decays $D_s^+ \to K_1(1270)^0 e^+ \nu_e$ and $D_s^+ \to b_1(1235)^0 e^+ \nu_e$ for the first time. No significant signals are observed for either decay mode. The upper limits on the (product) branching fractions are determined to be $\mathcal{B}[D_s^+ \to K_1(1270)^0 e^+ \nu_e] < 4.1 \times 10^{-4}$ and $\mathcal{B}[D_s^+ \to b_1(1235)^0 e^+ \nu_e] \cdot \mathcal{B}[b_1(1235)^0 \to \omega\pi^0] < 6.4 \times 10^{-4}$ at 90% confidence level.

DOI: 10.1103/PhysRevD.108.112002

I. INTRODUCTION

In the standard model (SM), semileptonic charmed meson decays provide an outstanding probe to explore the dynamics of both weak and strong interactions in the charm sector [1]. Compared to the semileptonic decays into pseudoscalar and vector mesons, charmed meson decays involving axial-vector mesons in the final state are not well-studied from either the experimental [2,3] or the theoretical [4–9] side. Extensive studies of the semileptonic charmed meson decays into axial-vector mesons $K_1(1270)$ and $b_1(1235)$ play an important role in the understanding of non-perturbative strong-interaction dynamics in weak decays [4–9]. BESIII and CLEO Collaborations have reported studies of $D^{0(+)} \to \bar{K}_1(1270) e^+ \nu_e$ [10–12]. The reported branching fractions are consistent with theoretical predictions based on the Isgur-Scora-Grinstein-Wise (ISGW) quark model [5] and its updated version (ISGW2) [6], as well as with those based on the covariant light-front quark model [4]. The BESIII Collaboration has also performed a search for $D^{0(+)} \to b_1(1235) e^+ \nu_e$, and no significant signal was observed [13]. For semileptonic D_s^+ decays into axial-vector mesons, no experimental study has been carried out so far.

The semileptonic decays of $D_s^+ \to K_1(1270)^0 e^+ \nu_e$ and $D_s^+ \to b_1(1235)^0 e^+ \nu_e$ can proceed via the Feynman diagrams shown in Fig. 1. Reference [4] has predicted the branching fraction of $D_s^+ \to K_1(1270)^0 e^+ \nu_e$ to be of order 10^{-4}. In contrast, the $D_s^+ \to b_1(1235)^0 e^+ \nu_e$ decay

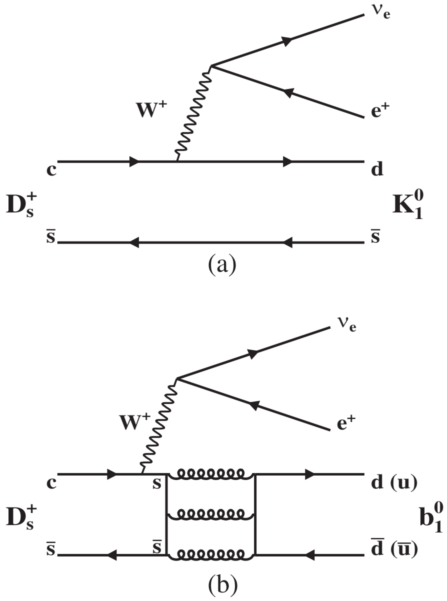

(a)

(b)

FIG. 1. Feynman diagrams of (a) $D_s^+ \to K_1(1270)^0 e^+ \nu_e$ and (b) $D_s^+ \to b_1(1235)^0 e^+ \nu_e$.

---

[a] Also at the Moscow Institute of Physics and Technology, Moscow 141700, Russia.

[b] Also at the Novosibirsk State University, Novosibirsk, 630090, Russia.

[c] Also at the NRC "Kurchatov Institute", PNPI, 188300, Gatchina, Russia.

[d] Also at Goethe University Frankfurt, 60323 Frankfurt am Main, Germany.

[e] Also at Key Laboratory for Particle Physics, Astrophysics and Cosmology, Ministry of Education; Shanghai Key Laboratory for Particle Physics and Cosmology; Institute of Nuclear and Particle Physics, Shanghai 200240, People's Republic of China.

[f] Also at Key Laboratory of Nuclear Physics and Ion-beam Application (MOE) and Institute of Modern Physics, Fudan University, Shanghai 200443, People's Republic of China.

[g] Also at State Key Laboratory of Nuclear Physics and Technology, Peking University, Beijing 100871, People's Republic of China.

[h] Also at School of Physics and Electronics, Hunan University, Changsha 410082, China.

[i] Also at Guangdong Provincial Key Laboratory of Nuclear Science, Institute of Quantum Matter, South China Normal University, Guangzhou 510006, China.

[j] Also at Frontiers Science Center for Rare Isotopes, Lanzhou University, Lanzhou 730000, People's Republic of China.

[k] Also at Lanzhou Center for Theoretical Physics, Lanzhou University, Lanzhou 730000, People's Republic of China.

[l] Also at the Department of Mathematical Sciences, IBA, Karachi 75270, Pakistan.

TABLE I. The integrated luminosities and requirements of $M_{\rm BC}$ for various energy points.

$E_{\rm cm}$ (GeV)	Luminosity (pb^{-1})	$M_{\rm BC}$ (GeV/c^2)
4.128	401.5	[2.010, 2.061]
4.157	408.7	[2.010, 2.070]
4.178	3189.0	[2.010, 2.073]
4.189	569.8	[2.010, 2.076]
4.199	526.0	[2.010, 2.079]
4.209	571.7	[2.010, 2.082]
4.219	568.7	[2.010, 2.085]
4.226	1091.7	[2.010, 2.088]

rate is highly suppressed due to isospin violation and the Okubo-Zweig-Iizuka (OZI) rule, so the weak annihilation effect in $D_s^+ \to b_1(1235)^0 e^+ \nu_e$ decay is relatively small. Experimental measurements of these two decay modes are important to test theoretical calculations and to understand nonperturbative effects in heavy meson decays.

In this article, we present the first search for $D_s^+ \to K_1(1270)^0 e^+ \nu_e$ and $D_s^+ \to b_1(1235)^0 e^+ \nu_e$ with $K_1(1270)^0 \to K^- \pi^+ \pi^0$ and $b_1(1235)^0 \to \omega \pi^0$, respectively. The charge conjugate channels are always implied throughout this paper. This analysis is performed by analyzing e^+e^- collision data corresponding to an integrated luminosity of 7.33 fb^{-1} [14] collected at eight center-of-mass energy ($E_{\rm cm}$) points, as listed in Table I, between 4.128 and 4.226 GeV with the BESIII detector.

II. BESIII DETECTOR AND MONTE CARLO SIMULATION

The BESIII detector [15] records symmetric e^+e^- collisions provided by the BEPCII storage ring [16] in the center-of-mass energy range from 2.0 to 4.95 GeV, with a peak luminosity of 1×10^{33} cm^{-2} s^{-1} achieved at $\sqrt{s} = 3.77$ GeV. BESIII has collected large data samples in this energy region [17]. The cylindrical core of the BESIII detector covers 93% of the full solid angle and consists of a helium-based multilayer drift chamber (MDC), a plastic scintillator time-of-flight system (TOF), and a CsI(Tl) electromagnetic calorimeter (EMC), which are all enclosed in a superconducting solenoidal magnet providing a 1.0 T magnetic field. The solenoid is supported by an octagonal flux-return yoke with resistive plate counter muon identification modules interleaved with steel. The charged-particle momentum resolution at 1 GeV/c is 0.5%, and the dE/dx resolution is 6% for electrons from Bhabha scattering. The EMC measures photon energies with a resolution of 2.5% (5%) at 1 GeV in the barrel (end cap) region. The time resolution in the TOF barrel region is 68 ps, while that in the end cap region is 110 ps. The end cap TOF system was upgraded in 2015 using multigap resistive plate chamber technology, providing a time resolution of 60 ps [18–20]; about 83% of the data used here benefits from this upgrade. Luminosity [14] at each energy point, with a total uncertainty of about 1.0%, is given in Table I.

Simulated data samples produced with a Geant4-based [21] Monte Carlo (MC) package, which includes the geometric description of the BESIII detector [22] and the detector response, are used to determine detection efficiencies and estimate backgrounds. The simulation models the beam energy spread and initial state radiation (ISR) in the e^+e^- annihilations with the generator KKMC [23]. Inclusive MC samples 40 times the size of data are used to simulate the background contributions. These samples, which contain no signal $D_s^+ \to K_1(1270)^0 e^+ \nu_e$ and $D_s^+ \to b_1(1235)^0 e^+ \nu_e$ decays, include the production of open charm processes, the ISR production of vector charmonium(-like) states, and the continuum processes incorporated in KKMC. The known decay modes are modeled with EvtGen [24,25] using branching fractions either taken from the Particle Data Group [2], and the remaining unknown decays from the charmonium states with LUNDCHARM [26,27]. Final state radiation (FSR) from charged final state particles is incorporated using the PHOTOS package [28]. The signal decays $D_s^+ \to K_1(1270)^0 e^+ \nu_e$ and $D_s^+ \to b_1(1235)^0 e^+ \nu_e$ are simulated using the ISGW2 model [6]. The $K_1(1270)^0$ is allowed to decay into all subdecays with the $K^- \pi^+ \pi^0$ final state and the branching fractions of $K_1(1270)^0$ subdecays quoted from PDG [2]. The $b_1(1235)^0$ decays into the $\omega \pi^0$ final state with $\omega \to \pi^+ \pi^- \pi^0$. A relativistic Breit-Wigner function is used to parametrize the resonances $K_1(1270)^0$ and $b_1(1235)^0$, whose masses and widths are fixed to the individual world-average values [2].

III. ANALYSIS METHOD

In the e^+e^- collision data taken at center-of-mass energies between 4.128 and 4.226 GeV, the $D_s^\pm$ mesons are produced mainly via the $e^+e^- \to D_s^{*\pm} D_s^\mp \to \gamma(\pi^0) D_s^+ D_s^-$ process. In the analysis we adopt the double-tag (DT) method pioneered by the MARK III Collaboration [29,30]. In single-tag (ST) candidates, the D_s^- meson is fully reconstructed via one of its hadronic decay modes. In a DT candidate, the transition $\gamma(\pi^0)$ from D_s^{*+} and the signal decay are successfully selected in the presence of a ST D_s^- meson. The branching fraction of the signal decay is determined by

$$\mathcal{B}_{\rm sig} = \frac{N_{\rm DT}}{N_{\rm ST}^{\rm tot} \cdot \bar{\epsilon}_{\gamma(\pi^0){\rm sig}}}, \tag{1}$$

where $N_{\rm DT}$ and $N_{\rm ST}^{\rm tot}$ are the yields of the DT events and of the ST D_s^- mesons, respectively; $\bar{\epsilon}_{\gamma(\pi^0){\rm sig}} = \sum_i (N_{\rm ST}^i \epsilon_{\rm DT}^i / \epsilon_{\rm ST}^i) / N_{\rm ST}^{\rm tot}$ is the effective signal efficiency of selecting the $\gamma(\pi^0)$ and the signal decay in the presence of the ST D_s^- meson, averaging the values obtained for each ith ST mode according to the corresponding yields of ST D_s^- mesons, where $\epsilon_{\rm ST}^i$ and $\epsilon_{\rm DT}^i$ are the detection efficiencies of the ST D_s^- mesons and the DT candidates (ST and DT efficiencies) for the ith ST mode, respectively.

IV. SINGLE TAG SELECTION

To reconstruct the candidates for ST D_s^-, we use thirteen hadronic decay modes: $D_s^- \to K^+K^-\pi^-$, $K^+K^-\pi^-\pi^0$, $\pi^+\pi^-\pi^-$, $K_S^0K^-$, $K_S^0K^-\pi^0$, $K_S^0K_S^0\pi^-$, $K_S^0K^+\pi^-\pi^-$, $K_S^0K^-\pi^+\pi^-$, $\eta_{\gamma\gamma}\pi^-$, $\eta_{\pi^+\pi^-\pi^0}\pi^-$, $\eta'_{\pi^+\pi^-\eta_{\gamma\gamma}}\pi^-$, $\eta'_{\gamma\rho^0}\pi^-$, and $\eta_{\gamma\gamma}\rho^-$. Throughout this paper, the ρ denotes $\rho(770)$ and the subscripts of $\eta^{(\prime)}$ denote the reconstructed decay modes.

All the charged tracks, except for those from the K_S^0 mesons, are required to originate from a region defined as $|\cos\theta| < 0.93$, $|V_{xy}| < 1$ cm and $|V_z| < 10$ cm, where θ is the polar angle with respect to the z axis (the MDC symmetry axis) $|V_{xy}|$ and $|V_z|$ are the distances of closest approach with respect to the interaction point (IP), in the transverse plane and along the z axis, respectively.

Particle identification (PID) of charged kaons and pions is implemented by combining dE/dx and TOF information. For charged kaon (pion) candidates, the likelihood for the kaon (pion) hypothesis is required to be larger than that for the pion (kaon) hypothesis.

The K_S^0 candidates are reconstructed via the $K_S^0 \to \pi^+\pi^-$ decay. The two charged pions are required to satisfy $|V_z| < 20$ cm and $|\cos\theta| < 0.93$. They are assumed to be $\pi^+\pi^-$ without any PID selection, and their invariant mass is required to be within $(0.486, 0.510)$ MeV/c^2. The decay length of the K_S^0 candidates from the IP is required to be greater than twice the vertex resolution, and this requirement suppress about 75% of background.

Photon candidates are identified using showers in the EMC. The deposited energy of each shower must be more than 25 MeV in the barrel region ($|\cos\theta| < 0.80$) and more than 50 MeV in the end cap region ($0.86 < |\cos\theta| < 0.92$). To exclude showers originating from charged particles, the angle subtended by the EMC shower and the position of the closest charged track at the EMC must be greater than 10° as measured from the IP. To suppress electronic noise and showers unrelated to the event, the difference between the EMC time and the event start time is required to be within [0, 700] ns.

The π^0 and $\eta_{\gamma\gamma}$ candidates are reconstructed from photon pairs with invariant masses being in the mass intervals (0.115, 0.150) and $(0.500, 0.570)$ GeV/c^2, respectively. A 1-constraint kinematic fit is performed on each selected photon pair, by constraining the invariant mass to the π^0 or η nominal mass [2]; to suppress the combinatorial background, $\chi^2 < 20$ is required. To select $\rho^{-(0)}$, $\eta_{\pi^0\pi^+\pi^-}$, $\eta'_{\eta\pi^+\pi^-}$, and $\eta'_{\gamma\rho^0}$ candidates, the invariant masses of the $\pi^-\pi^{0(+)}$, $\pi^0\pi^+\pi^-$, $\eta\pi^+\pi^-$, and $\gamma\rho^0$ combinations are required to be within the mass intervals $(0.570, 0.970)$ GeV/c^2, $(0.530, 0.570)$ GeV/c^2, $(0.946, 0.970)$ GeV/c^2 and $(0.940, 0.976)$ GeV/c^2, respectively. In addition, for $\eta'_{\gamma\rho^0}$ the energy of the γ is required to be greater than 0.1 GeV.

The low momentum pions from D^{*+} decays are suppressed by requiring the momentum of any pion not from K_S^0, η, or η' decays to be greater than 0.1 GeV/c. In order to reject the peaking background from $D_s^- \to K_S^0\pi^-$ in the selection of $D_s^- \to \pi^+\pi^-\pi^-$, the invariant mass of any $\pi^+\pi^-$ combination is required to be outside the mass window $(0.468, 0.528)$ GeV/c^2.

The backgrounds from non-$D_s^\pm D_s^{*\mp}$ processes are suppressed by using the beam-constrained mass of the ST D_s^- candidates, defined as

$$M_{\rm BC} \equiv \sqrt{E_{\rm beam}^2/c^4 - |\vec{p}_{\rm ST}|^2/c^2}, \tag{2}$$

where $E_{\rm beam}$ is the beam energy and $\vec{p}_{\rm ST}$ is the momentum of the ST D_s^- candidate in the e^+e^- rest frame. The $M_{\rm BC}$ is required to be within the intervals listed in Table I [31,32]. This requirement retains most of the D_s^- and D_s^+ mesons from $e^+e^- \to D_s^{*\mp}D_s^\pm$.

If there are multiple candidates present per ST mode per charge, only the one with the D_s^- recoil mass,

$$M_{\rm rec} \equiv \sqrt{\left(E_{\rm cm} - \sqrt{|\vec{p}_{\rm ST}|^2c^2 + m_{D_s^-}^2c^4}\right)^2/c^4 - |\vec{p}_{\rm ST}|^2/c^2}, \tag{3}$$

closest to the D_s^{*+} nominal mass [2] is kept for further analysis. The invariant mass distributions ($M_{\rm ST}$) of the accepted ST candidates for each mode are shown in Fig. 2 for the data sample at $E_{\rm cm} = 4.178$ GeV. For each ST mode, the yields of reconstructed D_s^- mesons are derived from fits to the individual $M_{\rm ST}$ distributions. In the fits, the signal is described by the shape obtained by signal MC simulation convolved with a Gaussian function to include the resolution difference between data and simulation. In the fit of the $D_s^- \to K_S^0K^-$ ST mode, the shape of the $D_s^- \to K_S^0\pi^-$ peaking background is modeled by the corresponding MC shape convolved with the same Gaussian function used for the signal shape, and the corresponding yield is left unconstrained. The combinatorial background is described by a second-order polynomial, as verified by analyzing the inclusive MC samples, whose parameters are left free in the fit. Figure 2 shows the fit results, where the black arrows indicate the selected $M_{\rm ST}$ signal regions. The candidates located in these signal regions are kept for further analysis.

The contribution from the $e^+e^- \to (\gamma_{\rm ISR})D_s^+D_s^-$ process has been estimated by MC simulation between 0.4% and 1.1%, and it has been subtracted to extract the final D_s^- yields. Table II summarizes, separately for each ST mode,

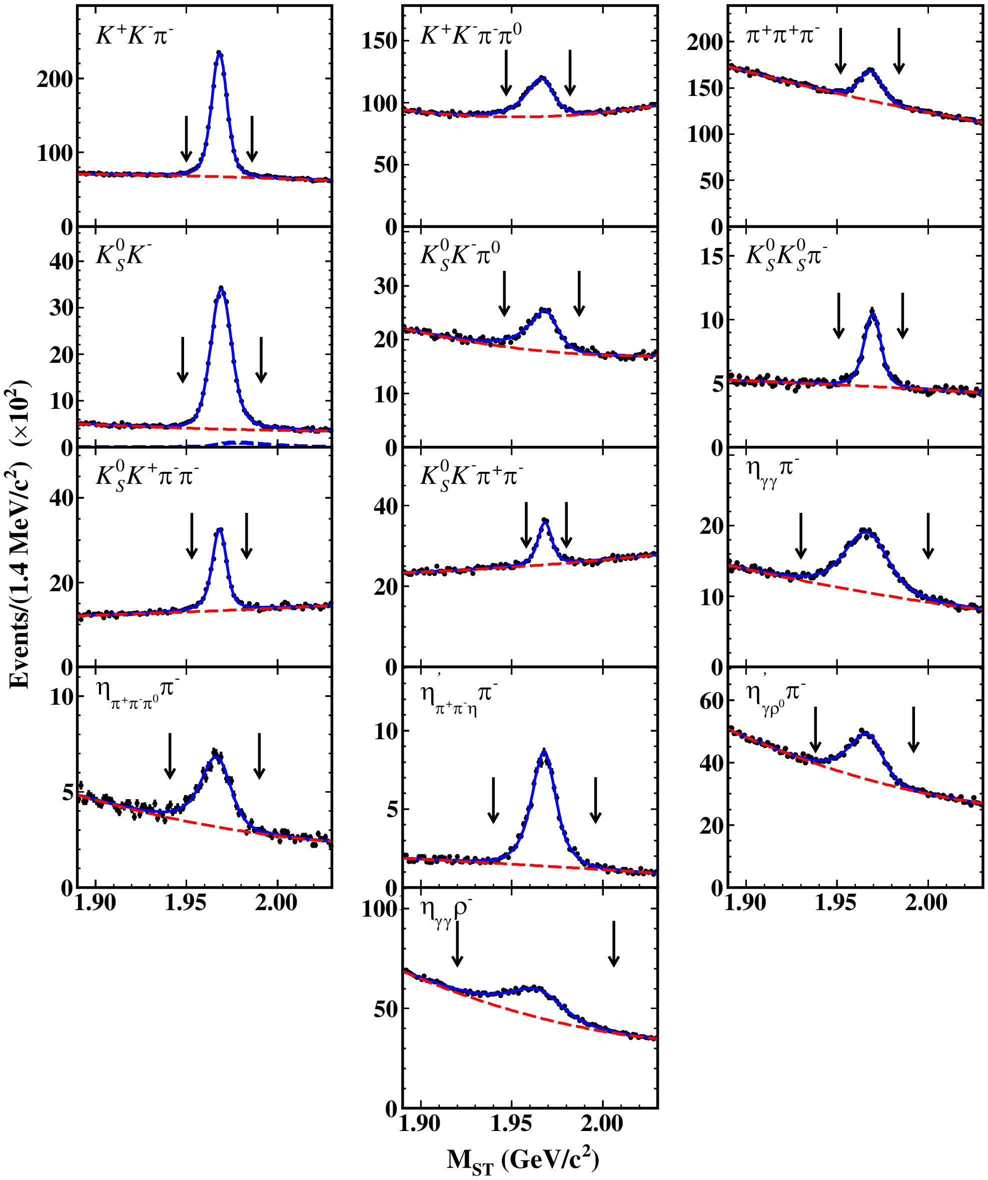

FIG. 2. Invariant mass distributions of the ST D_s^- candidates for each ST mode, from the data sample at $E_{\rm cm} = 4.178$ GeV. The points with error bars denote the data, the blue solid curves represent the best fit results, and the red dashed curves stand for the fitted backgrounds. For the $D_s^- \to K_S^0 K^-$ ST mode, the blue dotted curve is the peaking background from $D^- \to K_S^0 \pi^-$. The arrows indicate the chosen $M_{\rm ST}$ signal regions.

the total yields of ST D_s^- mesons ($N_{\rm ST}$), obtained summing up all the energy points, together with the average ST efficiencies $\epsilon_{\rm ST} = N_{\rm ST}/\sum_j (N^j_{\rm ST}/\epsilon^j_{\rm ST})$, where $N^j_{\rm ST}$ and $\epsilon^j_{\rm ST}$ are the corresponding ST D_s^- yield and ST efficiency for the j-th energy point, respectively.

V. DT SELECTION

To reconstruct DT events, the transition photon or π^0 in the system recoiling against the ST D_s^- is required. If more than one γ or π^0 candidate is present in the event, only the combination with the smallest energy difference $|\Delta E|$ with $\Delta E \equiv E_{\rm ST} + E^{\rm rec}_{\gamma(\pi^0)+D_s^-} + E_{\gamma(\pi^0)} - E_{\rm cm}$, is retained, where $E^{\rm rec}_{\gamma(\pi^0)+D_s^-} \equiv \sqrt{|\vec{p}_{\gamma(\pi^0)} + \vec{p}_{\rm ST}|^2 c^2 + m^2_{D_s^+} c^4}$, E_i and $\vec{p}_i$ ($i = \gamma(\pi^0)$ or ST) are the energy and momentum of $\gamma(\pi^0)$ or ST D_s^- in the rest initial e^+e^- frame, respectively.

In the presence of a ST D_s^- and a transition $\gamma(\pi^0)$, the signal decay candidates are selected with the remaining tracks as follows. There must be exactly three charged tracks available. One of the tracks with charge opposite to that of the ST D_s^- is identified as the positron. The other two oppositely charged tracks are identified as kaon and pion for $D_s^+ \to K_1(1270)^0 e^+ \nu_e$, or two pions for

TABLE II. The yields of ST D_s^- mesons ($N_{\rm ST}$) and the average ST efficiencies ($\epsilon_{\rm ST}$) for the complete data sample. Uncertainties are statistical only. The efficiencies do not include the branching fractions of the daughter particle decays.

Tag mode	$N_{\rm ST}$ ($\times 10^3$)	$\epsilon_{\rm ST}$ (%)
$K^+K^-\pi^-$	280.7 ± 0.9	40.87 ± 0.01
$K^+K^-\pi^-\pi^0$	86.3 ± 1.3	11.83 ± 0.01
$\pi^-\pi^+\pi^-$	72.7 ± 1.4	51.86 ± 0.03
$K_S^0K^-$	62.2 ± 0.4	47.37 ± 0.03
$K_S^0K^-\pi^0$	23.0 ± 0.6	17.00 ± 0.03
$K_S^0K_S^0\pi^-$	10.4 ± 0.2	22.51 ± 0.05
$K_S^0K^+\pi^-\pi^-$	29.6 ± 0.3	20.98 ± 0.03
$K_S^0K^-\pi^+\pi^-$	15.3 ± 0.4	18.23 ± 0.03
$\eta_{\gamma\gamma}\pi^-$	39.6 ± 0.8	48.31 ± 0.04
$\eta_{\pi^+\pi^-\pi^0}\pi^-$	11.7 ± 0.3	23.31 ± 0.05
$\eta'_{\pi^+\pi^-\eta}\pi^-$	19.7 ± 0.2	25.17 ± 0.04
$\eta'_{\gamma\rho^0}\pi^-$	50.1 ± 1.0	32.46 ± 0.03
$\eta_{\gamma\gamma}\rho^-$	80.1 ± 2.3	19.92 ± 0.01

$D_s^+ \to b_1(1235)^0e^+\nu_e$. The selection criteria of kaons and pions are the same as those used in selecting the ST D_s^- candidates. The pion candidate must have charge opposite to that of the positron for $D_s^+ \to K_1(1270)^0e^+\nu_e$. To form a $K_1(1270)^0$ candidate, the $K^+\pi^-\pi^0$ invariant mass is required to be within $(1.158, 1.358)$ GeV/c^2. For the $D_s^+ \to \pi^+\pi^-\pi^0\pi^0e^+\nu_e$ candidates, there are always two possible $\pi^+\pi^-\pi^0$ combinations to form the ω: the candidate is kept for further analysis if either or both of the combinations has an invariant mass falling in the ω mass signal region of $(0.757, 0.807)$ GeV/c^2. To form a $b_1(1235)^0$ candidate, the $\omega\pi^0$ invariant mass is required to be within $(1.080, 1.380)$ GeV/c^2.

The e^+ PID uses dE/dx, TOF, and EMC information to construct likelihoods for the electron, pion, and kaon hypotheses ($\mathcal{L}_e$, $\mathcal{L}_\pi$, and $\mathcal{L}_K$). The e^+ candidate is required to satisfy $\mathcal{L}_e > 0.001$ and $\mathcal{L}_e/(\mathcal{L}_e + \mathcal{L}_\pi + \mathcal{L}_K) > 0.8$. Its deposited energy in the EMC is required to be greater than 0.75 and 0.80 times its momentum reconstructed by the MDC for $D_s^+ \to K_1(1270)^0e^+\nu_e$ and $D_s^+ \to b_1(1235)^0e^+\nu_e$, respectively, to further suppress the background from misidentified hadrons and muons.

The signal candidates are examined by the kinematic variable $\mathrm{U}_{\rm miss} \equiv |E_{\rm cm} - E_{\rm ST} - E_{\gamma(\pi^0)} - E_h - E_e| - |-\vec{p}_{\rm ST} - \vec{p}_{\gamma(\pi^0)} - \vec{p}_h - \vec{p}_e|c$, where E_k and $\vec{p}_k$ ($k = e$ or h) are the energy and momentum of the e^+ or the hadron [$K_1(1270)$ or $b_1(1235)$] in the e^+e^- rest frame. To improve the $\mathrm{U}_{\rm miss}$ resolution, the candidate tracks, along with the missing neutrino, are subjected to a kinematic fit requiring energy and momentum conservation. In addition, the invariant mass of each $D_s^\pm$ meson is constrained to the nominal known $D_s^\pm$ mass, the invariant mass of the $D_s^+\gamma(\pi^0)$ or $D_s^-\gamma(\pi^0)$ combination to the known $D_s^{*\pm}$ mass, and the combination with the lowest χ^2 is kept. This kinematic fit is only used to improve resolution and no event is rejected. For correctly reconstructed signal events, $\mathrm{U}_{\rm miss}$ peaks at zero.

To suppress backgrounds from D_s^+ hadronic decays, the maximum energy of the unused showers, $E_{\gamma\rm extra}^{\rm max}$, must be less than 0.3 GeV and 0.2 GeV for $D_s^+ \to K_1(1270)^0e^+\nu_e$ and $D_s^+ \to b_1(1235)^0e^+\nu_e$, respectively, optimized with the Punzi method [33] using the inclusive MC samples. The DT candidate events with additional charged tracks ($N_{\rm extra}^{\rm char}$) or additional π^0 candidates, $N_{\rm extra}^{\pi^0} \neq 0$, are removed.

Figure 3 shows the $\mathrm{U}_{\rm miss}$ distributions of the selected candidate events in data. Unbinned maximum likelihood fits are performed on these distributions. In the fits, the signal and background are modeled by the simulated shapes obtained from the signal MC events and the inclusive MC samples, respectively, and the yields of the signal and background are left free. Since no significant signal is observed, upper limits will be set by

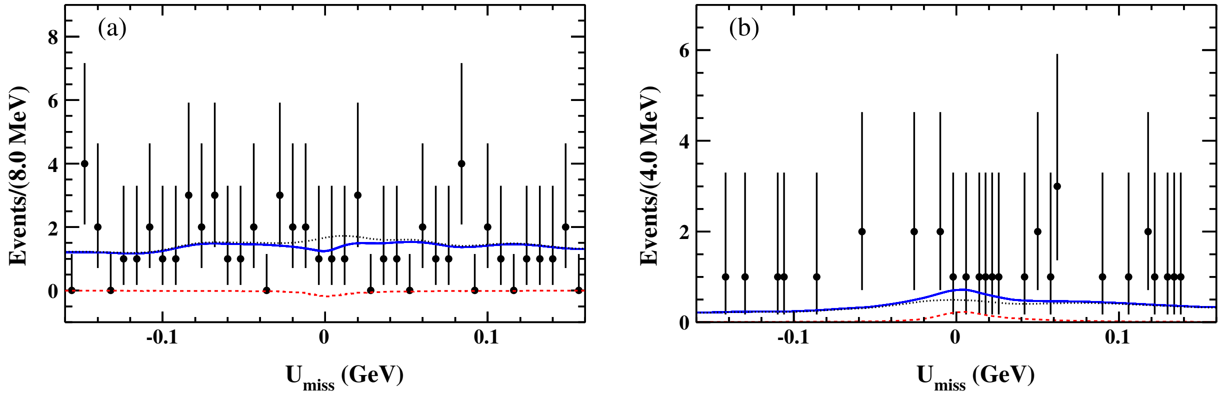

FIG. 3. Fits to the $\mathrm{U}_{\rm miss}$ distributions of the (a) $D_s^+ \to K_1(1270)^0e^+\nu_e$ and (b) $D_s^+ \to b_1(1235)^0e^+\nu_e$ candidate events. The points with error bars are data, the red dashed curve is the signal, the black dotted curve is the background contribution, and the blue solid curve shows the total fit.

TABLE III. The DT efficiencies ($\epsilon_{\rm DT}$) and the effective signal efficiencies ($\epsilon_{\gamma(\pi^0){\rm sig}}$) for various ST modes. The uncertainties are statistical only. All the efficiencies are given in % and do not include the branching fractions of the daughter particle decays.

Tag mode	$\epsilon_{{\rm DT},K_1}$	$\epsilon_{\gamma(\pi^0){\rm sig},K_1}$	$\epsilon_{{\rm DT},b_1}$	$\epsilon_{\gamma(\pi^0){\rm sig},b_1}$
$K^+K^-\pi^-$	3.10 ± 0.03	7.58 ± 0.08	1.19 ± 0.01	2.92 ± 0.03
$K^+K^-\pi^-\pi^0$	0.78 ± 0.03	6.57 ± 0.24	0.28 ± 0.01	2.34 ± 0.07
$\pi^-\pi^+\pi^-$	4.21 ± 0.04	8.13 ± 0.09	1.67 ± 0.02	3.22 ± 0.04
$K_S^0K^-$	3.78 ± 0.05	7.98 ± 0.11	1.54 ± 0.02	3.25 ± 0.05
$K_S^0K^-\pi^0$	1.31 ± 0.04	7.74 ± 0.22	0.47 ± 0.02	2.78 ± 0.12
$K_S^0K_S^0\pi^-$	1.62 ± 0.06	7.19 ± 0.26	0.58 ± 0.03	2.56 ± 0.13
$K_S^0K^+\pi^-\pi^-$	1.33 ± 0.05	6.33 ± 0.23	0.51 ± 0.02	2.43 ± 0.09
$K_S^0K^-\pi^+\pi^-$	1.28 ± 0.05	7.02 ± 0.27	0.42 ± 0.02	2.28 ± 0.12
$\eta_{\gamma\gamma}\pi^-$	4.06 ± 0.04	8.40 ± 0.09	1.67 ± 0.03	3.45 ± 0.06
$\eta_{\pi^+\pi^-\pi^0}\pi^-$	1.83 ± 0.03	7.84 ± 0.15	0.70 ± 0.02	2.98 ± 0.14
$\eta'_{\pi^+\pi^-\eta}\pi^-$	1.86 ± 0.03	7.39 ± 0.13	0.71 ± 0.02	2.83 ± 0.10
$\eta'_{\gamma\rho^0}\pi^-$	2.63 ± 0.04	8.10 ± 0.14	1.00 ± 0.02	3.07 ± 0.06
$\eta_{\gamma\gamma}\rho^-$	1.83 ± 0.06	9.19 ± 0.28	0.66 ± 0.01	3.30 ± 0.07

assuming all the fitted signals are from $K_1(1270)^0$ or $b_1(1235)^0$.

Table III summarizes the average DT efficiencies and the effective signal efficiencies for various ST modes, respectively. The average DT efficiency for each ST mode are averaged over the yields of ST D_s^- mesons at the different energy points. The averaged signal efficiencies $\bar{\epsilon}_{\gamma(\pi^0){\rm sig}}$ are 0.0773 ± 0.0005 and 0.0295 ± 0.0002 for $D_s^+ \to K_1(1270)^0 e^+ \nu_e$ and $D_s^+ \to b_1(1235)^0 e^+ \nu_e$, respectively.

VI. SYSTEMATIC UNCERTAINTY

In setting the upper limit branching fractions, the systematic uncertainties are divided into efficiency independent and dependent parts.

A. Efficiency independent systematic uncertainty

The efficiency independent systematic uncertainty originates from the fit to the U$_{\rm miss}$ distribution of the signal D_s^+ decay candidates. It affects the signal yield determination and is dominated by the uncertainty from imperfect knowledge of the background shape. The uncertainty associated with the signal shape is negligible. This systematic uncertainty is studied by altering the nominal MC background shape with two methods. First, alternative MC samples are used to determine the background shape, where the relative fractions of backgrounds from $q\bar{q}$, non-$D_s^{*+}D_s^-$ open charm are varied within their uncertainties. Second, the background shape is obtained from the inclusive MC samples using a kernel estimation method [34] implemented in RooFit [35]. The smoothing parameter of RooKeysPdf is varied between 0 and 2 to obtain alternative background shapes.

TABLE IV. Efficiency dependent systematic uncertainties of (a) $D_s^+ \to K_1(1270)^0 e^+ \nu_e$ and (b) $D_s^+ \to b_1(1235)^0 e^+ \nu_e$. All the uncertainties are given in %.

Sources	(a)	(b)
$N_{\rm ST}$	0.5	0.5
$K^\pm$, $\pi^\pm$ tracking	2.0	2.0
$K^\pm$, $\pi^\pm$ PID	2.0	2.0
$e^\pm$ tracking	1.0	1.0
$e^\pm$ PID	1.0	1.0
π^0 reconstruction	2.0	4.0
$\gamma(\pi^0)$ from D_s^{*+}	1.0	1.0
$E_{\gamma\,{\rm extra}}^{\rm max}$, $N_{\rm extra}^{\rm char}$ and $N_{\rm extra}^{\pi^0}$	2.6	2.6
ω mass window	⋯	1.2
$K_1^0(1270)$, $b_1^0(1235)$ mass windows	1.5	0.9
MC statistics	0.8	0.7
$\mathcal{B}$ of K_1 or ω decays	10.7	0.8
Signal model	1.1	1.0
Total	11.8	6.2

B. Efficiency dependent systematic uncertainty

The efficiency dependent systematic uncertainties in the measurement of the branching fractions are listed in Table IV.

The uncertainty associated with the ST yield $N_{\rm ST}$ is estimated to be 0.5%, from the change of the $N_{\rm ST}^{\rm tot}$ yield when modifying the angle of MC-truth association for the signal shape and changing the order of the polynomial for the background shape. The uncertainties associated with the efficiencies of $e^\pm$ tracking (PID), $K^\pm$ tracking (PID), $\pi^\pm$ tracking (PID), and π^0 reconstruction are investigated using data and MC samples of $e^+e^- \to \gamma e^+e^-$ events [36] and $e^+e^- \to K^+K^-\pi^+\pi^-$ [37]. The systematic uncertainties from the tracking (PID) efficiencies are assigned as 1.0% per $K^\pm$, $\pi^\pm$, or $e^\pm$. The π^0 reconstruction efficiencies include photon finding, the π^0 mass window, and the 1-constraint kinematic fit, and the corresponding systematic uncertainty is estimated as 2.0% per π^0 [37].

The uncertainty from the selection of the transition $\gamma(\pi^0)$ from D_s^{*+} with the least $|\Delta E|$ method is estimated to be 1.0% by using the control samples of $D_s^+ \to K^+K^-\pi^+$ and $D_s^+ \to \eta\pi^+\pi^0$ [38]. The uncertainties of the $E_{\gamma\,{\rm extra}}^{\rm max}$, $N_{\rm extra}^{\pi^0}$, and $N_{\rm extra}^{\rm char}$ requirements are estimated to be 2.6% by analyzing DT $D_s^+D_s^-$ events. The systematic uncertainty associated with the ω mass window is assigned to be 1.2% using a control sample of $D^0 \to K_S^0\omega$ [13].

The systematic uncertainties related to the $K_1(1270)^0$ and $b_1(1235)^0$ mass windows are estimated using alternative signal MC samples, which are produced by varying the mass and width of the $K_1(1270)^0$ and $b_1(1235)^0$ by $\pm 1\sigma$. The maximum changes of the signal efficiencies, 1.5% and 0.9%, are assigned as the systematic uncertainties for $D_s^+ \to K_1(1270)^0 e^+ \nu_e$ and $D_s^+ \to b_1(1235)^0 e^+ \nu_e$,

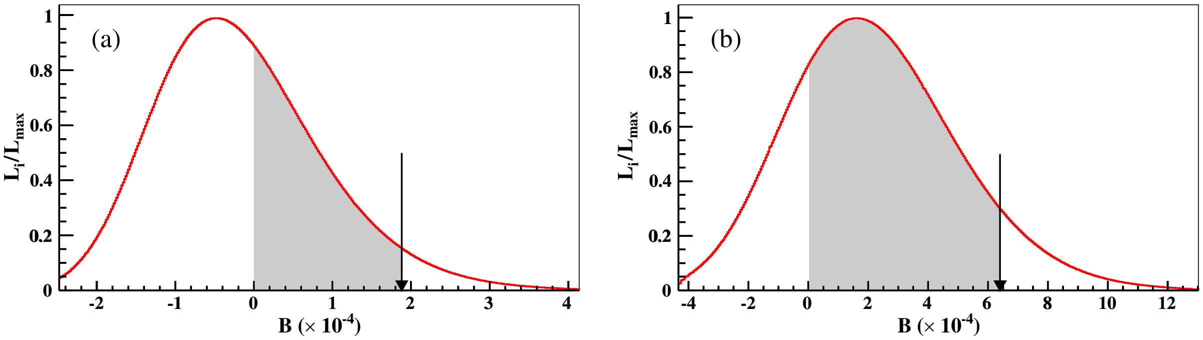

FIG. 4. The distributions of likelihood versus the corresponding branching fraction products of (a) $D_s^+ \to K_1(1270)^0 e^+ \nu_e$ and (b) $D_s^+ \to b_1(1235)^0 e^+ \nu_e$. The black arrows correspond to the upper limits at the 90% confidence level.

respectively. The uncertainties due to MC statistics, propagated from those of the ST and DT efficiencies, are 0.8% and 0.7% for $D_s^+ \to K_1(1270)^0 e^+ \nu_e$ and $D_s^+ \to b_1(1235)^0 e^+ \nu_e$, respectively.

The uncertainty from the quoted branching fraction of the $K_1(1270)^0 \to K^+ \pi^- \pi^0$ decay is estimated as 10.7% [2,39]; for the $b_1(1235)^0$ decay the $\omega \to \pi^+ \pi^- \pi^0$ uncertainty of 0.8% [2] is considered for the analysis.

The uncertainties due to the signal model are estimated to be 1.1% and 1.0% for $D_s^+ \to K_1(1270)^0 e^+ \nu_e$ and $D_s^+ \to b_1(1235)^0 e^+ \nu_e$, respectively, by comparing the DT efficiencies obtained from the nominal and phase space models, and varying the relative fractions of different K_1 subdecays.

By adding these uncertainties in quadrature, the total efficiency dependent systematic uncertainties, σ_ϵ, obtained are 11.8% and 6.2% for $D_s^+ \to K_1(1270)^0 e^+ \nu_e$ and $D_s^+ \to b_1(1235)^0 e^+ \nu_e$, respectively.

VII. RESULTS

To take into account the efficiency independent systematic uncertainty, the maximum-likelihood fits are repeated using different alternative background shapes as mentioned in the previous section and the one resulting in the most conservative upper limit is chosen. Finally, the second kind of systematic uncertainty σ_ϵ is incorporated in the calculation of the upper limit via [40,41]

$$L(\mathcal{B}) \propto \int_0^1 L\left(\mathcal{B}\frac{\epsilon}{\epsilon_0}\right) \exp\left[\frac{-(\epsilon-\epsilon_0)^2}{2\sigma_\epsilon^2}\right] d\epsilon, \qquad (4)$$

where $L(\mathcal{B})$ is the likelihood distribution as a function of assumed branching fraction; ϵ is the expected efficiency and ϵ_0 is the averaged MC-estimated efficiency. The likelihood distributions incorporating the systematic uncertainties are shown in Fig. 4.

The upper limits on the product of branching fractions at 90% confidence level, obtained by integrating $L(\mathcal{B})$ from zero to 90% of the total curve, are

$$\mathcal{B}[D_s^+ \to K_1^0 e^+ \nu_e] \cdot \mathcal{B}[K_1^0 \to K^+ \pi^- \pi^0] < 1.9 \times 10^{-4}$$

and

$$\mathcal{B}[D_s^+ \to b_1^0 e^+ \nu_e] \cdot \mathcal{B}[b_1^0 \to \omega \pi^0] < 6.4 \times 10^{-4},$$

where the numbers in the particle notations are omitted for brevity. Considering the branching fraction of $\mathcal{B}[K_1(1270)^0 \to K^+ \pi^- \pi^0] = 0.467 \pm 0.050$ [2,39], we set an upper limit on

$$\mathcal{B}[D_s^+ \to K_1(1270)^0 e^+ \nu_e] < 4.1 \times 10^{-4}$$

at 90% confidence level, which is comparable with the theoretical prediction in Ref. [4].

VIII. SUMMARY

In summary, by analyzing 7.33 fb^{-1} of e^+e^- collision data collected at E_{cm} between 4.128 and 4.226 GeV with the BESIII detector, we search for the semileptonic decays $D_s^+ \to K_1(1270)^0 e^+ \nu_e$ and $D_s^+ \to b_1(1235)^0 e^+ \nu_e$ for the first time. No significant signal is observed for both the decays. The upper limits on the (product) branching fractions are determined to be $\mathcal{B}[D_s^+ \to K_1(1270)^0 e^+ \nu_e] < 4.1 \times 10^{-4}$ and $\mathcal{B}[D_s^+ \to b_1(1235)^0 e^+ \nu_e] \cdot \mathcal{B}[b_1(1235)^0 \to \omega \pi^0] < 6.4 \times 10^{-4}$ at 90% confidence level.

ACKNOWLEDGMENTS

The BESIII Collaboration thanks the staff of BEPCII and the IHEP computing center for their strong support. This work is supported in part by National Key R&D Program of China under Contracts No. 2020YFA0406400 and No. 2020YFA0406300; National Natural Science Foundation of China (NSFC) under Contracts No. 12205175, No. 11635010, No. 11735014, No. 11835012, No. 11935015, No. 11935016, No. 11935018, No. 11961141012, No. 12022510, No. 12025502, No. 12035009, No. 12035013, No. 12061131003, No. 12192260, No. 12192261, No. 12192262, No. 12192263, No. 12192264, No. 12192265, No. 12221005, No. 12225509, and No. 12235017; the Chinese Academy of Sciences (CAS) Large-Scale Scientific Facility Program; the CAS Center for Excellence in Particle Physics (CCEPP); CAS Key Research Program of Frontier Sciences under Contracts No. QYZDJ-SSW-SLH003 and No. QYZDJ-SSW-SLH040; 100 Talents Program of CAS; The Institute of Nuclear and Particle Physics (INPAC) and Shanghai Key Laboratory for Particle Physics and Cosmology; ERC under Contract No. 758462; The project ZR2019BA036 supported by Shandong Provincial Natural Science Foundation, China; European Union's Horizon 2020 research and innovation programme under Marie Sklodowska-Curie Grant agreement under Contract No. 894790; German Research Foundation DFG under Contracts No. 443159800 and No. 455635585, Collaborative Research Center CRC 1044, FOR5327, GRK 2149; Istituto Nazionale di Fisica Nucleare, Italy; Ministry of Development of Turkey under Contract No. DPT2006K-120470; National Research Foundation of Korea under Contract No. NRF-2022R1A2C1092335; National Science and Technology fund of Mongolia; National Science Research and Innovation Fund (NSRF) via the Program Management Unit for Human Resources & Institutional Development, Research and Innovation of Thailand under Contract No. B16F640076; Polish National Science Centre under Contract No. 2019/35/O/ST2/02907; The Swedish Research Council; U.S. Department of Energy under Contract No. DE-FG02-05ER41374.

[1] H. B. Li and X. R. Lyu, Natl. Sci. Rev. **8**, nwab181 (2021).

[2] R. L. Workman *et al.* (Particle Data Group), Prog. Theor. Exp. Phys. **2022**, 083C01 (2022).

[3] B. C. Ke, J. Koponen, H. B. Li, and Y. H. Zheng, Annu. Rev. Nucl. Part. Sci. **73**, 285 (2023).

[4] H. Y. Cheng and X. W. Kang, Eur. Phys. J. C **77**, 587 (2017); **77**, 863(E) (2017).

[5] N. Isgur, D. Scora, B. Grinstein, and M. B. Wise, Phys. Rev. D **39**, 799 (1989).

[6] D. Scora and N. Isgur, Phys. Rev. D **52**, 2783 (1995).

[7] R. Khosravi, K. Azizi, and N. Ghahramany, Phys. Rev. D **79**, 036004 (2009).

[8] Y. B Zuo, Y. Hu, L. L. He, W. Yang, Y. Chen, and Y. N. Hao, Int. J. Mod. Phys. A **31**, 1650116 (2016).

[9] S. Momeni and R. Khosravi, J. Phys. G **46**, 105006 (2019).

[10] M. Ablikim *et al.* (BESIII Collaboration), Phys. Rev. Lett. **123**, 231801 (2019).

[11] M. Ablikim *et al.* (BESIII Collaboration), Phys. Rev. Lett. **129**, 131801 (2021).

[12] M. Artuso *et al.* (CLEO Collaboration), Phys. Rev. Lett. **99**, 191801 (2007).

[13] M. Ablikim *et al.* (BESIII Collaboration), Phys. Rev. D **102**, 112005 (2020).

[14] M. Ablikim *et al.* (BESIII Collaboration), Chin. Phys. C **39**, 093001 (2015); **46**, 113002 (2022).

[15] M. Ablikim *et al.* (BESIII Collaboration), Nucl. Instrum. Methods Phys. Res., Sect. A **614**, 345 (2010).

[16] C. H. Yu *et al.*, *Proceedings of IPAC2016, Busan, Korea, 2016*, 10.18429/JACoW-IPAC2016-TUYA01.

[17] M. Ablikim *et al.* (BESIII Collaboration), Chin. Phys. C **44**, 040001 (2020).

[18] X. Li *et al.*, Radiat. Detect. Technol. Methods **1**, 13 (2017).

[19] Y. X. Guo *et al.*, Radiat. Detect. Technol. Methods **1**, 15 (2017).

[20] P. Cao *et al.*, Nucl. Instrum. Methods Phys. Res., Sect. A **953**, 163053 (2020).

[21] S. Agostinelli *et al.* (Geant4 Collaboration), Nucl. Instrum. Methods Phys. Res., Sect. A **506**, 250 (2003).

[22] K. X. Huang *et al.*, Nucl. Sci. Tech. **33**, 142 (2022).

[23] S. Jadach, B. F. L. Ward, and Z. Was, Phys. Rev. D **63**, 113009 (2001); Comput. Phys. Commun. **130**, 260 (2000).

[24] D. J. Lange, Nucl. Instrum. Methods Phys. Res., Sect. A **462**, 152 (2001).

[25] R. G. Ping, Chin. Phys. C **32**, 599 (2008).

[26] J. C. Chen, G. S. Huang, X. R. Qi, D. H. Zhang, and Y. S. Zhu, Phys. Rev. D **62**, 034003 (2000).

[27] R. L. Yang, R. G. Ping, and H. Chen, Chin. Phys. Lett. **31**, 061301 (2014).

[28] E. Richter-Was, Phys. Lett. B **303**, 163 (1993).

[29] R. M. Baltrusaitis *et al.* (MARK III Collaboration), Phys. Rev. Lett. **56**, 2140 (1986).

[30] J. Adler *et al.* (MARK III Collaboration), Phys. Rev. Lett. **60**, 89 (1988).

[31] M. Ablikim *et al.* (BESIII Collaboration), Phys. Rev. D **107**, 032011 (2023).

[32] M. Ablikim *et al.* (BESIII Collaboration), Phys. Rev. D **104**, 032001 (2021).

[33] Giovanni Punzi, arXiv:2011.11770.

[34] K. S. Cranmer, Comput. Phys. Commun. **136**, 198 (2001).

[35] R. Brun and F. Rademakers, Nucl. Instrum. Methods Phys. Res., Sect. A **389**, 81 (1997).

[36] M. Ablikim *et al.* (BESIII Collaboration), Phys. Rev. D **106**, 112004 (2022).

[37] M. Ablikim *et al.* (BESIII Collaboration), Phys. Rev. D **99**, 091101(R) (2019).

[38] M. Ablikim *et al.* (BESIII Collaboration), Phys. Rev. Lett. **122**, 071802 (2019).

[39] $\mathcal{B}[K_1 \to K^+\pi^-\pi^0] = (2/3)\mathcal{B}[K_1 \to \rho K] + (4/9)\mathcal{B}[K_1 \to K^*(892)\pi] + (4/9)(0.93)\mathcal{B}[K_1 \to K_0^*(1430)\pi]$, where K_1 denotes $K_1(1270)^0$.

[40] K. Stenson, arXiv:physics/0605236.

[41] X. X. Liu, X. R. Lyu, and Y. S. Zhu, Chin. Phys. C **39**, 113001 (2015).